

Efficient Fluorescence Resonance Energy Transfer in Highly Stable Liposomal Nanohybrid Cerasome

Zhifei Dai,^{a*} Wenjie Tian,^b Xiuli Yue,^c Zhaozhu Zheng,^a Jingjing Qi,^a Naoto Tamai,^{d*} Jun-ichi Kikuchi^{e*}

Experimental Section

Preparation of nanocerasome linked with J-aggregates of cyanine dyes: 7 ml of aqueous dye solution is added to 3.4 mg of cerasome forming lipid. The suspension is then agitated using vortex mixer until a homogeneous milky suspension is obtained. The major component at this point is multilamellar vesicles (MLVs) that have an average size of several hundred nanometers. Then, the MLV dispersion is sonicated with a probe-type sonicator at 30 W for 3 min in the pulse mode at >23°C. The sonicated solution is left for at least 12 h at room temperature to allow hydrolysis to produce cerasomes with Si-O-Si networks.

Fourier transform infrared (FT-IR) spectra: FT-IR spectra of cerasomes were acquired using a Varian Resolution Fourier transform infrared spectrometer (Varian FTS 3100, USA). Samples were prepared in the forms of potassium bromide (KBr) disk. Approximately 1 mg sample and 99 mg of KBr powder was blended and triturated with agate mortar and pestle. The mixture was compacted using an IR hydraulic press at a pressure of 8 tons for 1 min. For each spectrum a 512-scan interferogram was collected with a 4 cm⁻¹ resolution from the 4000 to 500 cm⁻¹ region at room temperature with nitrogen gas.

Morphological characterization: The morphology of cerasomes was assessed using a scanning electron microscope (SEM) (Hitachi S-4500) and transmission electron microscope (TEM)(JEOL 2010 microscope operated at 200 kV). Atomic force microscopy (AFM) images were obtained by means of a Digital Instruments Nanoscope III in tapping mode (Digital Instrument Inc., Santa Barbara, CA).

Dynamic light scattering (DLS): The hydrodynamic diameter (D_{hy}) and polydispersity index of cerasomes were determined by a 90Plus/BI-MAS dynamic light scattering (DLS) analyzer (Brookhaven Instruments Co., U.S.A).

Absorption and fluorescence measurements: Absorption spectroscopy was performed using a Varian Cary 50 UV/Vis spectrophotometer between 200 and 800 nm by means of quartz cuvettes. Fluorescence spectra were obtained using a Varian Cary Eclipse spectrometer. All measurements were performed on air-equilibrated solutions at 25 °C.

Calculation of fluorescence quantum yield (ϕ): The increase of the acceptor fluorescence or the quenching of the donor fluorescence due to FRET were calculated by integration of the fluorescence intensity (I_{fl}) over the energy ($\tilde{\nu}$), obtaining the relative number of emitted light photons (N_i) for each step.

$$N_i = \int I_{\text{fl}} d\tilde{\nu} \quad (1)$$

Fluorescence quantum yield (ϕ_i) could be calculated by the following equation using $\phi_0 = 0.38$ ($\lambda_{\text{exc}} = 402$ nm) of TC J-aggregates adsorbed to poly(allylamine hydrochloride) (PAH) as standard for the quantum yield of the transferred or quenched energy according to the literature:^[14]

$$\phi_i = \phi_0 \frac{N_i}{N_0} \quad (2)$$

where N_0 is the number of emitted photons of the adsorbed TC dye in the absence of TCC under the excitation of 410 nm light, respectively. The experimental error in ϕ_i is typically 20%.

Picosecond lifetime measurements: The luminescence lifetime of samples was measured by a picosecond single-photon timing system equipped with a frequency doubled femtosecond cavity dumped Ti:Sapphire laser ($\lambda_{\text{ex}}=410$ nm, Kapteyn-Murnane Laboratories Inc.) as a excitation light source. Single photon counting technique was comprised a constant fraction discriminator (CFD, Tenelec TC 454), delay units (EG & G ORTEC, Model DB 463) and a time-to-amplitude converter (TAC, Tenelec TC 864) operated in reverse start stop mode and a data card running on PC. The detector was a microchannel plate photomultiplier (Hamamatsu, MCP R2809U), thus the overall temporal time resolution of the system was 40 ps. The quality of fit was judged in terms of a DW parameter, weighted residuals and reduced χ^2 values.

Results

The formation of siloxane bonds on the cerasome surface was proved by Fourier

transform infrared (FT-IR) spectroscopy (Fig.S1). Stretching bands assigned to the Si-O-Si and Si-OH groups were observed around 1100 and 920 cm^{-1} , respectively. The former peak intensity was much stronger than the latter in cerasomes in the dry state. Thus it is suggested that the cerasomes have a silicalike surface with siloxane frameworks.

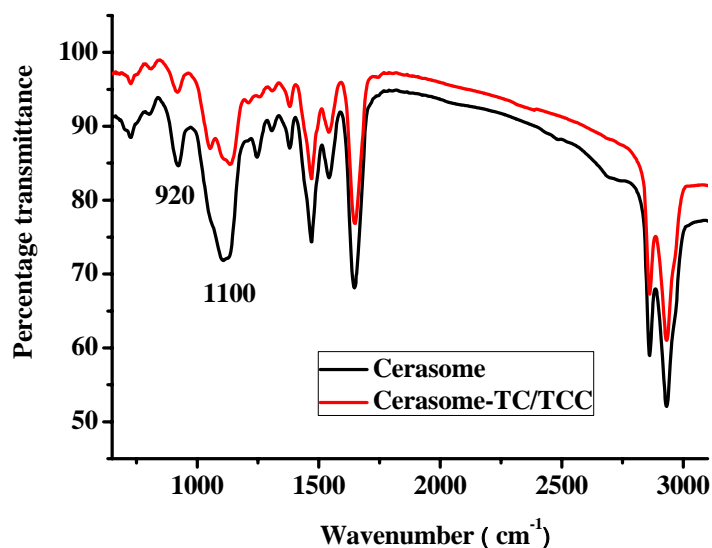


Fig. S1 FT-IR spectroscopy of cerasomes.

The morphology of the cerasomes were observed by transmission electron microscopy (TEM)(Fig.S2), scanning electron microscopy (SEM)(Fig.S3) and atomic force microscopy (AFM)(Fig.S4), respectively. The electron micrographs and AFM micrographs showed the presence of cerasomes with an average diameter of ca. 60 nm. The vesicular vesicular size was well consistent with the hydrodynamic diameter as evaluated by dynamic light scattering (DLS) measurements (Fig.S5).

The resulting cerasome (partially ceramic- or silica-coated liposome) solution showed high stability. After being stored at room temperature for three months, no notable change was observed in the appearance and sizes from AFM micrographs (Fig.S4) and dynamic light scattering (DLS) measurements for freshly prepared cerasomes and cerasomes after 3 months (Fig.S5) .

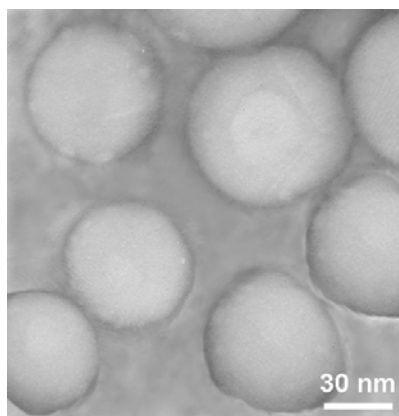


Fig. S2 TEM image of cerasome linked J-aggregates of cyanines.

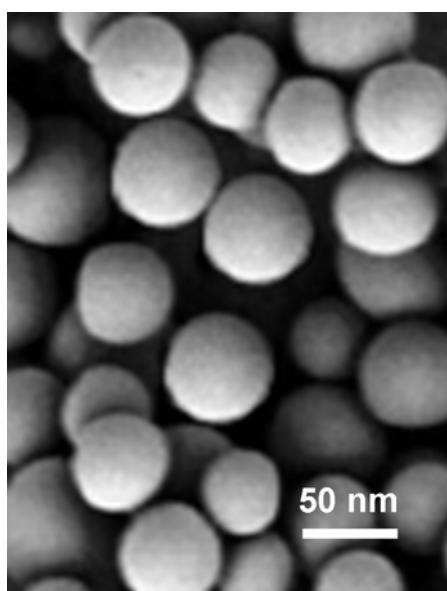
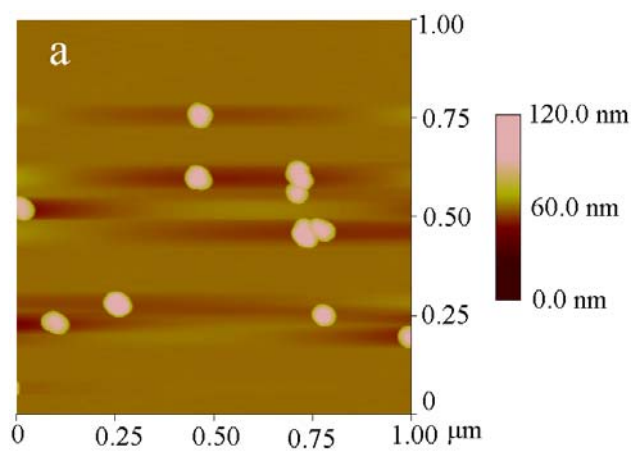


Fig. S3 SEM image of cerasome linked J-aggregates of cyanines.



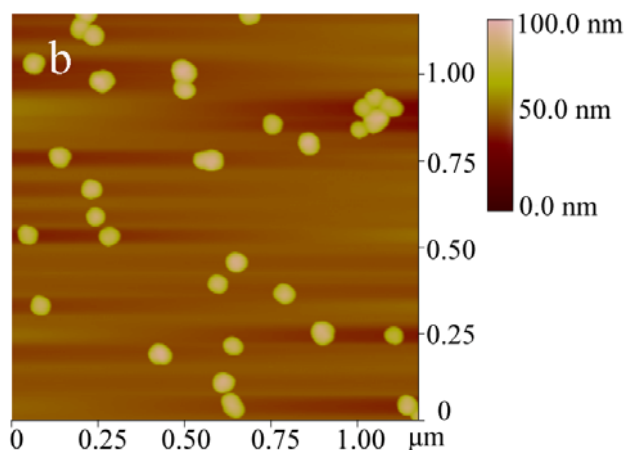


Fig. S4 AFM images of cerasomes for freshly prepared cerasomes (a) and cerasomes after 3 months (b).

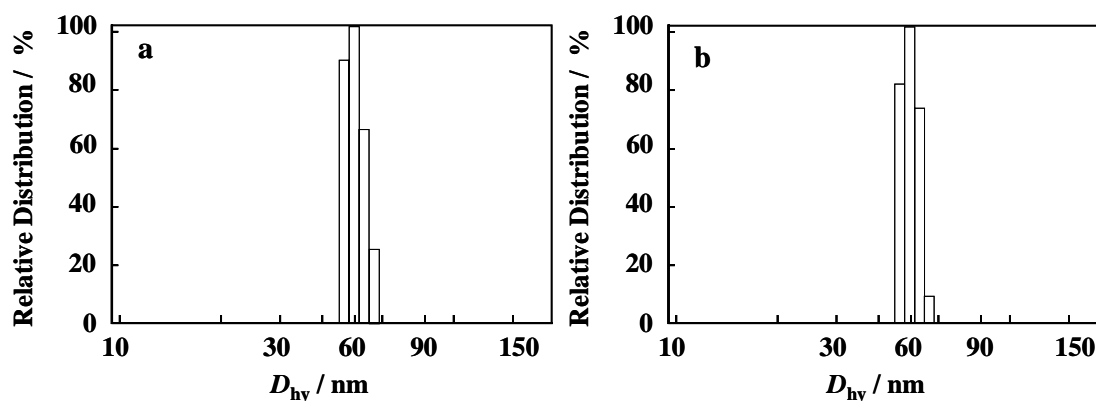


Fig. S5 Size distribution profiles by DLS measurements for freshly prepared cerasomes (a) and cerasomes after 3 months (b).

It is convenient to use surfactant solubilization to evaluate morphological stability of liposomes in aqueous media. The resistance of cerasomes against a cationic surfactant cetyltrimethylammonium bromide (CTAB) was determined by the light scattering intensity of the vesicles and conventional liposomes from dimyristoylphosphatidylcholine (DMPC) was used as a reference, as shown in Fig.S6. When three equivalents of CTAB were added to the DMPC liposome, the light scattering intensity was drastically decreased indicating a collapse of the vesicle. On the contrary, the cerasome exhibited remarkable morphological resistance toward CTAB. The light scattering intensity of the cerasome incubated for 24 h did not change at all even in the presence of 30 equivalents

of CTAB. It provided a strong evidence that the morphological stability of the bilayer vesicles was enhanced obviously through modification of molecular design of the cerasome-forming lipids.

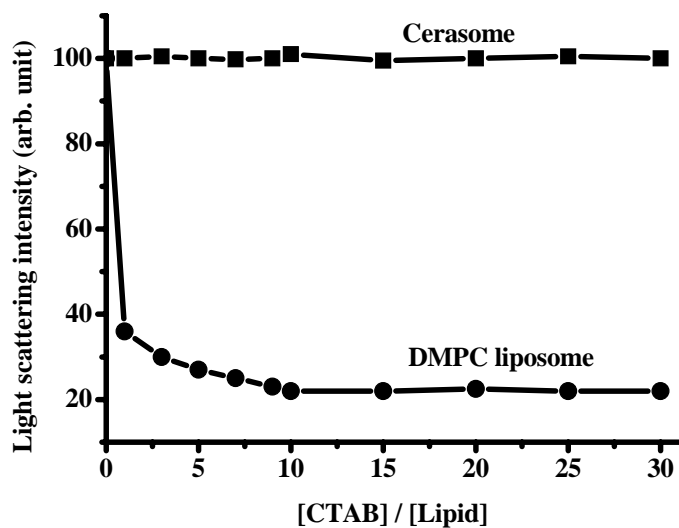


Fig. S6 Light scattering intensities of the cerasomes and DMPC-liposome as a function of added equivalents of CTAB: (■) cerasome incubated for 24 h; (●) DMPC-liposome.